CHAPTER VIII

SURFACE ENHANCED RAMAN SCATTERING OF 1,4-DIMETHOXY -3–BROMOMETHYLANTHRACENE-9,10-DIONE (DMBMAD) BY Ag NPs

Abstract

Ag NPs were prepared by solution combustion method with glycine as fuel. SERS of 1,4-dimethoxy-3-bromomethylanthracene -9,10 dione (DMBMAD) adsorbed on Ag NPs has been investigated. The orientation of DMBMAD on Ag NPs has been inferred from nRs and SERS spectral features. The observed spectral feature corroborated that DMBMAD would adsorb on Ag NPs by 'stand-on' orientation through the high intensity of C-H in-plane bending mode, C-Br stretching, ring stretching and C=O. In present case, the DMBMAD molecule and Ag NPs as component molecules for energy gap analysis, where as DMBMAD serve as donor and Ag NPs as acceptor. The calculated HOMO and LUMO energy gap shows that charge transfer occur within molecule and Ag NPs.

8.1 Introduction

Anthrodione (AD) is the most important quinone derivative of anthracene. Plants containing anthrodione have been used for millennia as dyestuffs and purgatives. Though quinones are found in plants and in a few animals, they usually are prepared by oxidation of aromatic amines, polyhydric phenols, and polynuclear hydrocarbons. Anthracene derivatives have various biomedical characteristics (bioactivities) and have the wide application for medicines, pesticides, etc [1,2].They are used principally in photographic dye chemicals, in medicines, as an antioxidant, in paints, varnishes, motor fuels, oils, pigments and in organic inhibitor. They play a vital role in paper industry as a catalyst to increase the pulp production yield and to improve the fiber strength through reduction reaction of cellulose to carboxylic acid [3, 4]. In this present investigation, SERS spectral analyses of DMBMAD molecule on Ag NPs were studied.

8.2. Experimental

8.2.1 Materials

The details of the chemicals used are similar as discussed in chapter IV and VI. DMBMAD was synthesized according to the literature [5].

8.2.2 Synthesis of Ag NPs using solution combustion method

Ag NPs used in this study were synthesized by solution combustion method as discussed in chapter II, IV and VI.

8.2.3 Characterization

The details of the instruments used are similar as described in chapter III.

8.3 Result and Discussion

8.3.1SERS Studies

8.3.1.1 Vibrational assignments

The structure of DMBMAD molecule is shown in figure 8.1. The nRs and SERS of DMBMAD are shown in figures 8.2 and 8.3 respectively. The observed vibrational modes and its corresponding assignments are listed in table 8.1. The equilibrium geometry and vibration wavenumber of the DMBMAD molecules in the electronic ground state have been computed at DFT/B3LYP level using the Gaussian 03. The calculated normal mode wave numbers of DMBMAD are listed in the table

8.1. In table 8.1 the description of vibration motion, such as bending, deformation, stretching etc, is on the basis of the vibration animations in the Gaussian view.

Generally, the carbonyl stretching mode falls in the region 1810-1600cm^{-1} [6]. In the present case the C=O stretching vibration were observed in the region 1784-1644cm^{-1} in both nRs and SERS. The C-C stretching vibrations in quinones usually appear in the region 1600-1250cm^{-1} [7]. When methyl group is substituted on the aromatic ring, the CH_3 deformation mode occurs in the region 1440-1360cm^{-1} [6]. In the present case, the C-C stretching modes were observed in the region 1609-1305cm^{-1} in both nRs and SERS. The nRs and SERS bands around 1467-1347cm^{-1} were assigned to C-C stretching mode of AD coupled with CH_3 deformation mode of methyl group. In AD, the C-H in-plane bending vibrations occur in the region 1300-1000cm^{-1} [8]. The CH_3 rocking vibrations usually appear in the region 1070-1010cm^{-1} [6]. The nRs bands in the region 1223-1067cm^{-1} and SERS bands in the region 1227-1013cm^{-1} were assigned to C-H in-plane bending vibrations. The nRs and SERS bands around 1067-1013cm^{-1} were due to the C-H in-plane bending vibrations mode of AD coupled with CH_3 rocking.The C-H out-of-plane bending modes of high intensity arises in the region 900-677cm^{-1} [9]. In the present case, the observed nRs bands around 962-688cm^{-1} and SERS bands at 964-722cm^{-1} were due to C-H out-of-plane vibrational modes. The skeletal deformation mode of AD molecule occurs in the region 600-250cm^{-1} [10]. The observed nRs band around 544-338cm^{-1} and SERS band around 603-340cm^{-1} were assigned to skeletal deformation of AD. In bromobenzene the band occurs at 267cm^{-1} is due to C-Br stretching modes and C-Br in-plane vibration mode occur in the region 152cm^{-1} [11]. In the present case a strong band is observed at 262cm^{-1} in nRs and SERS band at 264cm^{-1} for C-Br stretching vibrations. The C-Br in-plane vibrational modes are also presented in table 8.1.

8.3.1.2 Orientation of DMBMAD molecule and DMBMAD molecule on Ag NPs

There are two possibilities of molecular adsorption on the metal surface, namely physisorption and chemisorptions. The spectrum of physisorbed molecules is practically the same as that of the free molecules with only small changes being observed for the bandwidth along intensity enhancement. This situation corresponds to a relatively large distance between metal surface and adsorbed molecules. When the molecules are chemisorbed there is an overlapping of the molecular and metal

orbitals. Then the molecular symmetry is affected and the position of the bands and their relative intensities are dramatically changed [12].

The orientation of the molecule on the surface was determined on the basis of surface selection rules. The adsorption mechanism of an adsorbate can be deduced from its SERS spectrum. The orientation of the adsorbate on the metal nanoparticles will depend on the active sites through which the interaction takes place. The chemically possible orientations of the DMBMAD molecule on the Ag NPs were lying down (flat-on) on the Ag NPs through bonding with the ring system or 'standing up' (end-on) with bonding through the pair of the electron of the oxygen in C=O group and bromines. These binding sites may lead to the adsorption of the molecule on the Ag NPs [13-15]. The orientation of an adsorbed molecule has been studied from different points of view. They are analyzed as given below.

The ring stretching vibrations are most prominent in the spectrum of AD and its derivatives are highly characteristic of aromatic ring. Medium intense bands in the general region 1600–1250cm^{-1} were assigned to ring stretching vibration [16]. The SERS wavenumber of the ring stretching vibration increased by less than 10cm^{-1} and their bandwidth decreases substantially when the molecule adsorb on the metal surface via their π system. The title compound shows ten ring stretching vibrational mode observed in the region 1609-1305cm^{-1} in both nRs and SERS. The bands at 1606, 1508 and 1347cm^{-1} in nRs are downshifted in the SERS spectrum and their bandwidths are hardly affected. It was clearly suggests that DMBMAD adsorbed on the Ag NPs in a 'stand–on' orientation. From the observed up-shifted peaks and its wavenumber, it was difficult to make orientation of the DMBMAD molecules on the Ag NPs using ring stretching vibrations.

In the case of aromatic molecules, the intensity of out-of-plane vibrational modes decreases substantially relative to the in-plane vibrational modes when the adsorbed orientation is altered from perpendicular to 'stand-on' orientation. In the case of DMBMAD, five bands in nRs and four bands in SERS were observed due to the out-of plane vibrational modes. Some of the out-of-plane vibrational modes are not observed in the SERS spectrum. The intensity of the peak at 962 and 920cm^{-1}in nRs is less than that of the peak at 964 and 924cm^{-1} in SERS. Similarly, the intensity of aromatic out-of-plane C-H bands with respect to the in-plane bending mode

decreases as the molecule is adsorbed on almost stand to the Ag NPs. The absence of the some out-of-plane vibrational modes also indicates that the probability of the absorption of the DMBMAD molecule in a 'stand-on' orientation is greater.

Another possible way in which the DMBMAD derivative 'stand-on' adsorption occurs on the Ag NPs is through the C=O. Generally, in quinones the C=O stretching vibrational band is very strong in intensity [17]. In the present case, four bands were observed in the region 1744-1644cm^{-1} in nRs and three bands are observed in the region 1784-1707cm^{-1} in SERS of DMBMAD molecule. The intensity of these peaks is strong in SERS. If the molecule is adsorbed on the metal nanoparticles through a C=O group, the intensity of this peak increases and the wavenumber is upshifted with respect to the same band in nRs. In the present study, DMBMAD can interact with Ag NPs through the pair of the oxygen atom of the C=O group. According to the surface selection rule when DMBMAD is adsorbed on Ag NPs through the pair electron of oxygen atom of the C=O group, the intensity of these modes should be more prominent due to the polarizability tensor is normal to the Ag NPs. In the present case the intensity of this peak increases and slightly upshifted in SERS. Therefore, in the case the probability of the adsorption of the DMBMAD molecule on silver nanoparticles through a C=O group is more. It is further seen that vibrations involving atoms that are close to the Ag NPs will be enhanced. When the wavenumber difference between Raman bands in the normal and SERS spectra is not more than 10cm^{-1}, the molecular plane will be perpendicular to the Ag NPs [18,19]. In the present case the difference between nRs and SERS not more than 10cm^{-1} wavenumber which also evidence that the DMBMAD has 'stand-on' orientations.

''Stand-on' orientation of the title molecule on the Ag NPs may be through the bromine atom. In the present case the band at 264 and 262cm^{-1} in SERS and nRs respectively were due to C-Br stretching vibrational. The C-Br in-plane bending vibration modes also occur in the region 160 and 158cm^{-1} in SERS and nRs. In both case these modes were enhanced in SERS and shifted by 2cm^{-1}. Considering the DMBMAD molecule oriented 'stand-on' to the Ag NPs, the C-Br bond and the normal to the surface are parallel.

The enhancement rocking modes, skeletal deformation of AD and CH_3 deformation further support the orientation of DMBMAD on Ag NPs is 'stand-on' orientation of the benzene ring moiety on a silver substrate.

8.4 HOMO-LUMO studies

Many organic molecules, containing conjugated π electrons characterized by large values of molecular hyperpolarizabilities, were analyzed by means of vibrational spectroscopy [20, 21]. In most of the cases, even in the absence of inversion symmetry, the strongest bands in the Raman spectrum are weak in the SERS spectra and vice versa. But the intermolecular charge transfer from the donor to acceptor group through a single-double bond conjugated path can include large variations of both the molecular dipole moment and the molecular polarizability. The experimental spectroscopic behaviour described above is well accounted for by *ab initio* calculations in π conjugated systems that predict exceptionally large SERS and Raman intensities for the some normal modes [22]. It is also observed in our title molecule; the bands in the Raman spectrum have their counterpart in SERS showing that relative intensities in Raman and SERS spectra are comparable resulting from the electron cloud movement through π conjugated frame work from electron donor to electron accepter groups. The analysis of the wave function indicates that the electron absorption corresponding to the transition from the ground to the excited state and mainly described by electron from the HOMO to the LUMO. The frontier orbital gap helps to characterize the chemical reactivity, optical polarizability and chemical hardness-softness of a molecule [23].

Surfaces for the frontier orbitals were drawn to understand the bonding scheme of the title compound. The calculated HOMO-LUMO energies gaps are 3.23eV. The chemical hardness and softness of a molecule is a good indication of the chemical stability of the molecule. The molecules having small energy gap are more polarizable because they need small energy to excitation. The LUMO of π natural, (i.e. benzene ring) is localized over the whole C-C bond. The HOMO is also localized over C-C bond. The molecular orbital are sketched in figure 8.4 (a) and (b). The HOMO-LUMO energy gap has been calculated by using DFT/B3LYP level reveals that the energy gap reflected the chemical activity of the molecule. LUMO as an electron acceptor represents the ability to obtain an electron, HOMO represents the ability to donate an electron. The donor molecules are attached to the acceptor molecules via carbonyl groups. Due to the chemisorptions of the DMBMAD with Ag NPs, the molecular orbital of the donor molecules are mixed with metallic band states. Certain orbital of donor molecules interact strongly with the acceptor molecules and are

responsible for the chemisorptions bond. The strong charge transfer interaction through π- conjugated bridge result in substantial ground state Donor- Acceptor (DA) mixing and the appearance of charge transfer band in the electron adsorption spectrum. By comparing both cases, energy band gap between HOMO-LUMO of DA mixing (1.16eV) is lower than that of donor molecule (3.23eV) which indicates leads to strong intermolecular interaction. The HOMO and LUMO energy gap explain the fact eventual charge transfer interaction is taking place within the molecule.

8.5 Conclusion

The orientation of DMBMAD adsorbed on Ag NPs was studied using SERS studies. Ag NPs were synthesized using a solution combustion method with glycine as fuel. The nRs and SERS spectral analysis reveals that the DMBMAD adsorbed 'stand-on' orientation on the Ag NPs. HOMO and LUMO energy gap explain the eventual charge transfer interactions taking place within molecule and Ag NPs has been also discussed.

Reference

[1] M. Umadevi, V. Ramakrishnan, J. Raman Spectrosc., 34 (2003) 13.

[2] J. Yang, A. Dass, A. Monem, M. Rawashdeh,C. Sotiriou Leventis, Chem. Mater., 16 (2004) 3457.

[3] M.S. Jahan, J.Tappi., 84 (2001) 1.

[4] Z. Li, J. Li, G.J. Kubes, J. Pulp. Paper. Sci., 28 (2002) 234.

[5] O. Khoumeri, M. Montana, T. Terme, P. Vanelle, Tetrahedron., 64 (2008) 11237.

[6] A. Fathia Alseroury, J. Basic and Appl Sci. 5 (2011) 611.

[7] J. P. Kalyani, N. Kalaiselvi, N. Muniyandi, J. Powder. Sources., 111 (2002) 232.

[8] M.Govindarajan, S. Periandy, K.Ganesan, J. chem., 7 (2010) 457.

[9] N.B. Colthup, L.H. Daly, S.E. Wilberley, *Intoduction to infrared and Raman spectroscopy*, Academic Press, Newyork, (1990).

[10] P.Gao, M.J. Weaver, J. Phys. Chem., 89 (1985) 5040.

[11] M. Arivazhagan, N.K. Kandasamy, G. Thilagavathi, Indian J. Pure & Appl Phys., 50 (2012) 299.

[12] A.G. Malshukov, Phys. Rept., 194 (1990) 343.

[13] M. Moskovits, J. Chem. Phys., 77 (1982) 4408.

[14] J.A. Creighton, Surf. Sci., 124 (1983) 209.

[15] B. Giese, D. McNaughton, J. Phys. Chem. B., 106 (2002) 1461.

[16] M.Umadevi, V. Ramakrishnan, Spectrochimi Acta. Part A., 58 (2002) 2941.

[17] R. Aroca, R.E. Clavijo, Spectrochim. Act. Part A., 44 (1988) 171.

[18] G. Levi, J. Patigny, J.P. Massault, J. Aubard, *Thirteenth International Conference on Raman Spectroscopy,* Wurzburg, 1992.

[19] X. Gao, J.P. Davies, M.J. Weaver, J. Phys. Chem. 94 (1990) 6858.

[20] N. Sundsraganesan, G. Elango, C. Meganathan, M. Kurt, Mol.Simulat., 35 (2009) 705.

[21] T. Vijayakumar, I. Hubert Joe, C.P. Reghunadhan Nair, V.S. Jayakumar, Chem. Phys., 343 (2008) 83.

[22] J. Chowdhury, Vib. Spectrosc., 52 (2010) 85.

[23] B. Kosar, C. Albayrak, Spectrochim. Acta A., 78 (2011) 160-167.

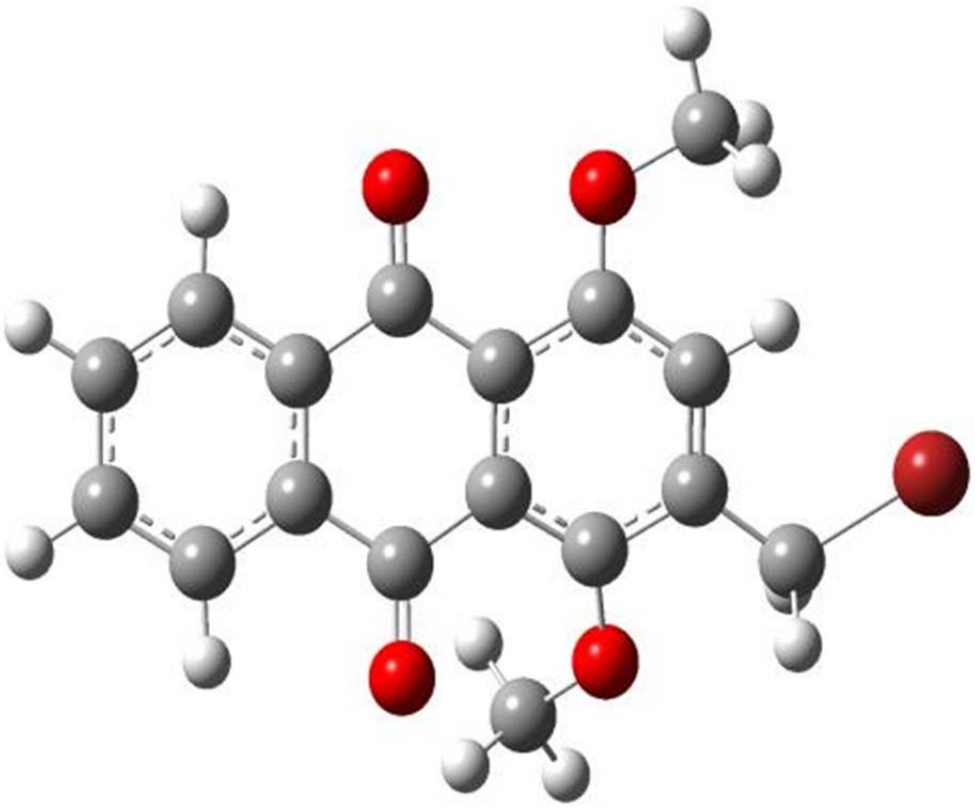

Figure 8.1 Structure of 1, 4-dimethoxy-3–bromomethylathracene-9,10- Dione (DMBMAD).

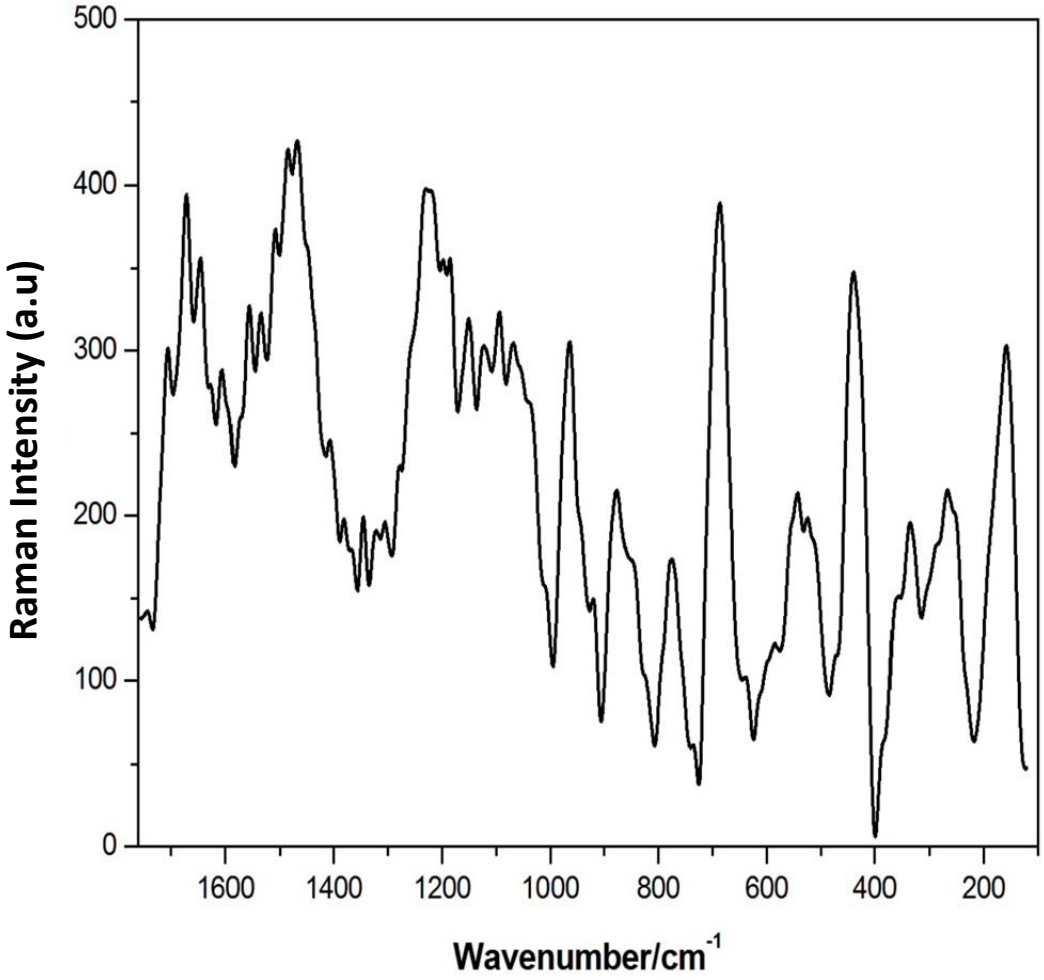

Figure 8.2 Normal Raman spectrums (nRs) spectra of DMBMAD molecule.

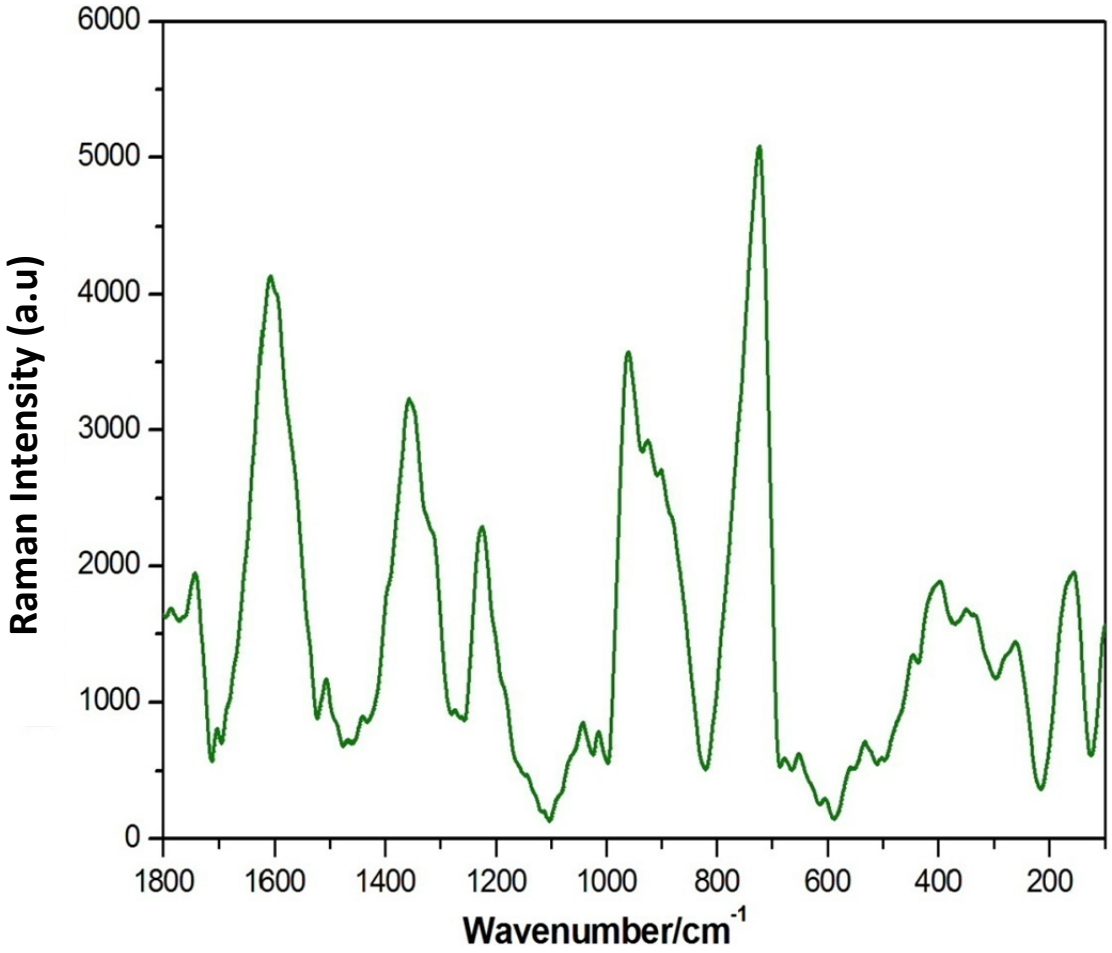

Figure 8.3 Surface Enhanced Raman (SERS) spectrums of DMBMAD on Ag NPs.

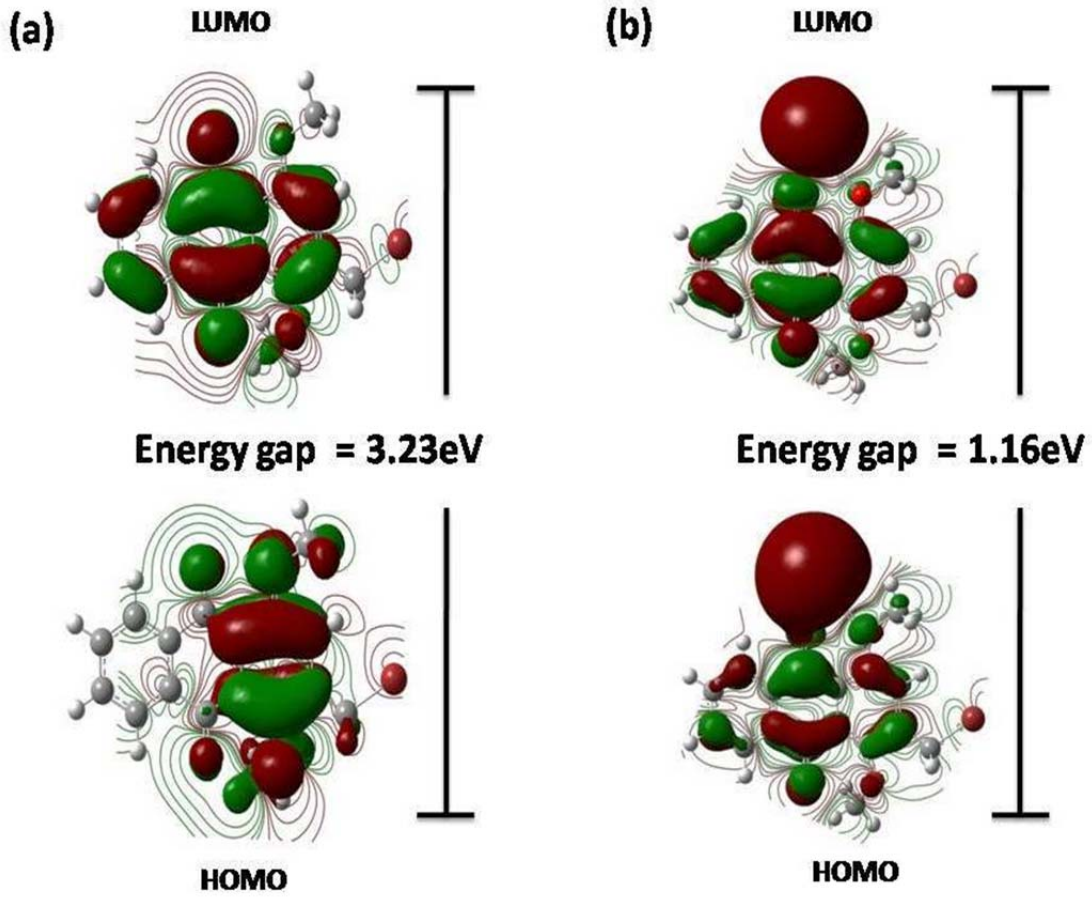

Figure 8.4 HOMO and LUMO plot of (a) DMBMAD and (b) DMBMAD on Ag NPs.

Table 8.1 Vibrational assignment of DMBMAD and DMBMAD on Ag NPs.

Calculated wavenumber cm^{-1}	Observed wavenumber (cm^{-1})		Band Assignments
	nRs	SERS	
		1784	(C=O) str.
	1744	1748	(C=O) str.
	1703	1707	(C=O) str.
1660	1670		(C=O) str.
1634	1644		(C=O) str.
1614	1606	1609	(C-C) str.
1572	1559		(C-C) str.
1525	1535		(C-C) str.
1500	1508	1510	(C-C) str.
1487	1488		(C-C) str.
1478	1467		(C-C) str., CH_3 def.
1392	1382		(C-C) str., CH_3 def.
1344	1347	1355	(C-C) str., CH_3 def.
	1323		(C-C) str.
1308	1305		(C-C) str.
1211	1223	1227	(C-H) i.p.
1187	1185		(C-H) i.p.
1146	1152		(C-H) i.p.
1119	1126		(C-H) i.p.
	1097		(C-H) i.p.
1064	1067		(C-H) i.p., CH_3 rock.
		1043	(C-H) i.p., CH_3 rock.
1023		1013	(C-H) ip, CH_3 rock
960	962	964	(C-H) o.p.
916	920	924	(C-H) o.p.
		903	(C-H) o.p.
874	876		(C-H) o.p.
774	779		(C-H) o.p.

709		722	(C-H) o.p.
667	688		(C-H) o.p.
614		603	skel. def. AD.
541	544	533	skel. def. AD.
532	523		skel. def. AD.
440	441	447	skel. def. AD.
386		398	skel. def. AD.
329	338	340	skel. def. AD.
274	262	264	C-Br str.
178	158	160	C-Br i.p.

str.- stretching, def. - deformation, i.p.- in-plane bending, o.p.- out-of-plane bending, rock.- rocking, skel.- skeletal.